

TMS COIL DESIGN: WIRE AND WINDING CONSIDERATIONS

Mehran Talebinejad¹, and Sam Musallam^{1,2}

¹Department of Electrical and Computer Engineering, and ²Department of Physiology
McGill University, Quebec, CANADA

INTRODUCTION

Transcranial magnetic stimulation (TMS) is a non-invasive method for stimulating neural tissue. An electric current in the stimulation coil produces a magnetic field that induces a flow of electric current in nearby neurons. TMS follows this fundamental principle and is well established in physiology, brain mapping and therapeutic applications [1]. Our goal is to miniaturize the coil to increase stimulation specificity to a level that would allow TMS to be part of a feedback system for neural prosthetic applications.

The simplest TMS coil is a circle, 5 to 15 cm in outer diameter that includes 5 to 50 turns [2]. TMS coil windings are usually made of insulated copper wire. Rapid TMS with conventional coils quickly results in heat especially for prolonged high speed stimulation. This is due to high frequency current that tends to the outside of the wire bundle and increases the eddy currents inside the coil [3]. This effect reduces the effective cross-sectional area of the coil, increasing the coil resistance, energy loss and heating. Coil cooling systems are generally required in such instances. Cooling system adds substantial weight and bulk. This has led to more elaborate and expensive designs using multi-stranded magnet wires.

Previous research on TMS coil investigated coil arrays, and winding methods; these studies show interesting results based on numerical computations [1, 2, 4]. However, the type of wire or winding can significantly reduce the undesirable effects of high currents [5].

In this paper, we studied the effects of wire type and winding on single TMS coils. Round, square and rectangular magnet wires, and braided and compacted *Litz* wires are compared in terms of "coil efficiency". Horizontal- and vertical-spiral windings are also compared in terms of magnetic field intensity. Results of a simulation study using finite element method are presented. Results show "coil efficiency" could be improved by the choice of wire and winding method.

METHODS

Finite element method simulation

In our experiments, finite element method magnetics (FEMM) v.4.2 was employed. The simulations are 2D axisymmetric.

The magnetic field intensity, and the eddy currents and the coil AC resistance are computed. Uniform 0.1 mm triangles were used for mesh generation and finite element method solution. Table 1, summarizes the simulation parameters.

TMS circuit

The TMS stimulation circuit is comprised of a high voltage source that charges a capacitor which is discharged into a TMS coil via a heavy gauge high conductive cable. This combination behaves like an oscillating RCL circuit, which could be represented as a sine wave.

In our experiments, an ideal 3 kA, 50 Hz sine current source is serially connected to the coil. This configuration simulates a typical rapid stimulation [1]. The inductance and resistance of the circuit are mainly imposed by the coil. There are some small resistive and inductive contributions from the connecting cables and the circuit which increase the overall AC resistance and change the pulse shape, that are not taken into account in these simulations. These fixed effects do not compromise the comparisons in this study.

Magnetic field intensity

The field intensity vector distanced from a typical filament of the coil is given by the Ampere's law in this form [3],

$$(1) \quad \nabla \times H = J,$$

where J is the current density vector running through the coil filament and H is the magnetic field intensity. H can be rewritten as partial differential equations of the form,

$$(2) \quad H_x = \frac{1}{\mu_0} \frac{\partial J}{\partial x}, \text{ and } H_y = \frac{1}{\mu_0} \frac{\partial J}{\partial y},$$

where μ_0 is a function of permeability and conductivity of the space surrounding a point and H is computed as,

$$(3) \quad H = \sqrt{H_x^2 + H_y^2}.$$

At each point given the permeability and coordinates for arbitrary current densities the magnetic field intensity H , could be approximated in the vicinity of (x,y) by solving the partial

differential equations of field components H_x , and H_y . The finite element method accurately computes such partial differential equations [4]. The source current density could be easily computed given the current source and cross-section of the coil which are dictated by the wire and winding.

Eddy currents

The total current density is comprised of the source current density from the external source as well as the induced eddy currents. In this study we compute the eddy currents inside the coil as a measure of skin effects and induced current that compromise coil efficiency in terms of heating and resistive loss. Consider the total current density inside the coil J_t as,

$$(4) \quad J_t = Re\{J_s + J_e\} + Im\{J_s + J_e\},$$

where J_s is the source current density and J_e is the eddy current density. After computing the magnetic field intensity the total current density could be computed using (1); imaginary part of the total current density could be used to approximate the eddy current density in this form [4],

$$(5) \quad J_e \sim Im\{J_s + J_e\}.$$

Wire

Typical magnet wires have three different cross-sectional shapes: round, square and rectangular.

In our experiments, we selected the dimensions of each wire to maintain a cross-sectional area of $\sim 10 \text{ mm}^2$. The round wire is a standard 3.15 mm diameter, the square wire is a standard 3.15x3.15 mm, and the rectangular wire is custom 1x10 mm. A 3 kA current source in a $\sim 10 \text{ mm}^2$ cross-sectional wire yields a source current density of $\sim 300 \text{ A}$.

Winding

Virtually any winding form is composed of horizontal- and/or vertical-spiral(s) which are two fundamental winding methods.

In our experiments, we consider multi-layer horizontal- and vertical-spirals with the maximum number of turns possible to fill a cylinder with d cm diameter and h cm height.

Litz wire

Litz wire is a form of multi-stranded wire in which the strands are individually insulated. Substantial improvements in the "coil efficiency" have been reported in other areas of research using *Litz* wire from its ability to reduce the eddy currents inside the coil [3, 5].

Braided Litz

Braided *Litz* wire is usually comprised of a few thousand single conductors insulated with a very thin film. The high number of strands can have very thin insulations as the current is divided between a large numbers of conductors. This type of wire is interesting and potentially useful for TMS coil. It may also be optimal as it has the smallest thickness among high voltage magnet wires rated for 3kA and above. Braided *Litz wire* could easily be put into rectangular shape resulting in a wire with a large cross-section but with the minimum thickness. Braided *Litz* wire could be also round, or square. Braided *Litz* wire is conventionally made of ultrafine $2 \text{ }\mu\text{m}^2$ wires [6]. In our experiments we use 5000 strands per 10 mm^2 for braided *Litz*; this is the maximum number of strands allowed considering the cross-section.

Compacted Litz

Compacted *Litz* is usually comprised of as few as 10 strands. This type of *Litz* wire has the advantage of being compact compared to the braided *Litz*. Braided *Litz* has air between the strands resulting in a larger required cross-section for a high voltage rating; compacted *Litz* has less air and thus smaller required cross-section for a rated voltage. The ratio of cross-section compacted/braided is usually 1/2. Similar to braided *Litz*, compacted *Litz* wire could also be round, square or rectangular. In our experiments we use 20 strands per 10 mm^2 for compacted *Litz*. This is the minimum number of strands required for rectangular *Litz* wire with 10 mm^2 in practice using $500 \text{ }\mu\text{m}^2$ wires [6].

Experimental sets

There are 4 possible coils that could be wind using 3 wires in this experiment (Figures 1 to 4):

- 1) Horizontal- or vertical-spiral with round wire due to symmetry.
- 2) Horizontal- or vertical-spiral with square wire due to symmetry.
- 3) Horizontal-spiral with rectangular wire.
- 4) Vertical-spiral with rectangular wire.

The source and eddy current densities inside the coil are measured 1 mm from the coil surface around the air core.

The field intensity outside the coil is measured on a contour placed 2 cm from the top of the coil representing the human tissue in the air.

Our experiments are based on filling a (d,h) cm, (5,5) cm cylinder (i.e., miniaturized for TMS) with the maximum number of turns when the inner diameter is 1 cm, a (6,5) cm cylinder, when the inner diameter is 2 cm and a (7,5) cm cylinder, when the inner diameter is 3 cm.

RESULTS

Figures 1 to 4, show the 2D cross-section of each coil and the surrounding field intensity. The value of the field intensity at sites of interest is presented in Table 1. Coil surface around the air core is experiencing the highest magnetic field intensity. This suggests the eddy currents in this site are also the highest.

Figure 5, shows the typical source and eddy current densities inside the coil when a single-strand wire is used. Figure 6, shows the typical source and eddy current densities inside the coil when a braided *Litz* wire is used.

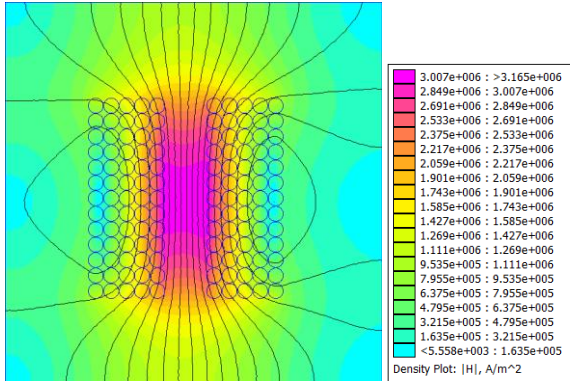


Figure 1: Spiral with round wire.

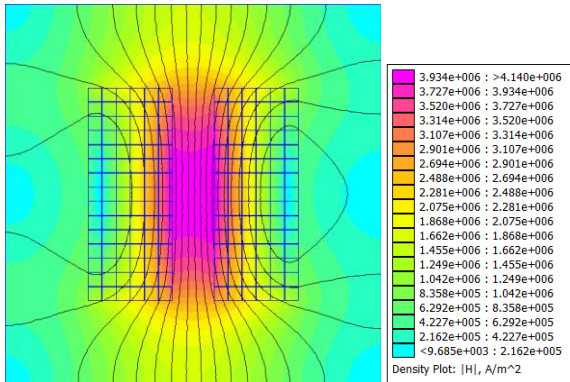


Figure 2: Spiral with square wire.

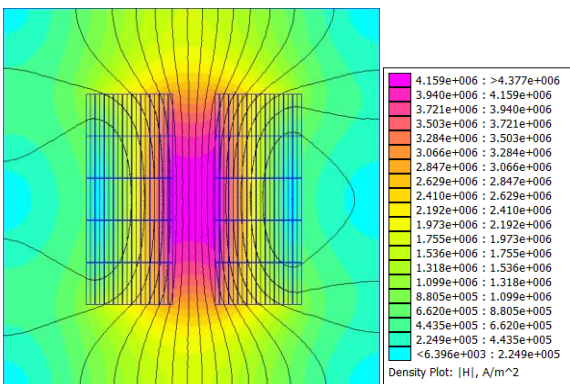


Figure 3: Horizontal-spiral with rectangular wire.

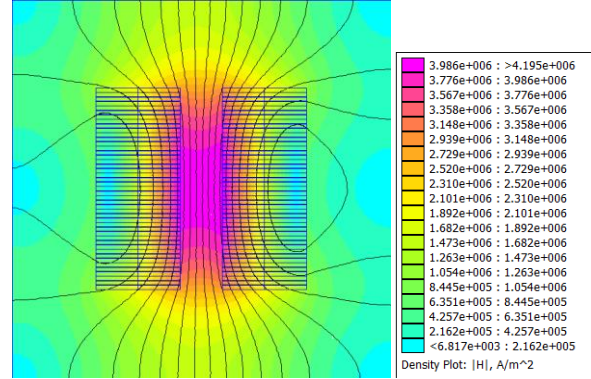


Figure 4: Vertical-spiral with rectangular wire.

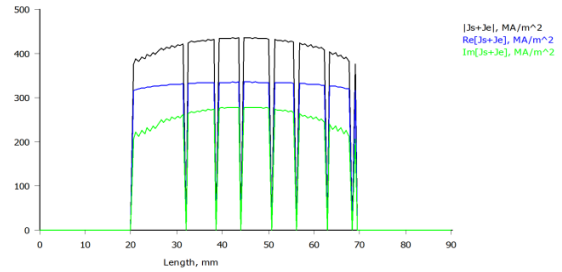


Figure 5: The source and eddy current densities are denoted as J_s and J_e , respectively. Typical single-strand wire, effects of J_e in green is influencing the overall current density. Zeroes are due to the air between the windings which has been set to 0.1 mm.

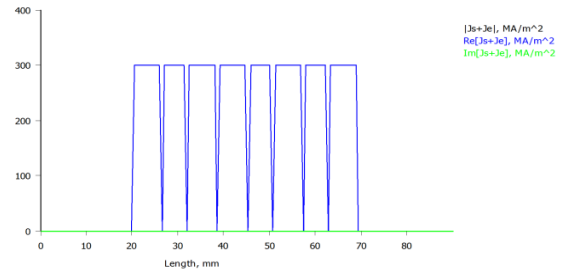


Figure 6: The effects of J_e are suppressed using *Litz* wire, $Im [J_s + J_e] \sim 0$.

Undesirable effects of eddy currents and an increased current density are noticeable in Figure 5. Suppressing effects of *Litz* wire on eddy currents are noticeable in Figure 6.

Table 1, summarizes all the simulation parameters and numerical results for each coil including ones with different inner diameters.

DISCUSSIONS

As shown in Table 1, the eddy currents are suppressed when either braided or compacted *Litz* wires were used compared to the single-strand wire. This could be explained by smooth distribution of current throughout the *Litz* wire cross-section [4].

As shown in Table 1, resistance of braided *Litz* is 5 times higher than compacted *Litz*. This means the compacted *Litz* outperforms the braided *Litz* in terms of resistive heating which degrades the “coil efficiency”.

The square and rectangular wires outperform the round wire in terms of winding; allow more windings in an equal space (i.e., tighter winding), which results in a greater magnetic intensity.

The rectangular wire slightly outperforms the square wire in terms of magnetic intensity. This could be also explained by the tighter winding with more turns.

Horizontal-spiral outperforms vertical-spiral in terms of magnetic intensity; this could be explained by the emphasis of stimulation on the coil’s number of turns on top of the coil; meanwhile, magnetic intensity is more in a wider area inside the vertical-spiral compared to the horizontal-spiral. Indeed, portable MRI resistive coil is a vertical-spiral exploiting this feature [8].

An increased inner diameter increases the magnetic intensity, but lowers the stimulation specificity.

CONCLUSIONS

This study shows the compacted rectangular *Litz* wire is potentially well-suited for TMS coil design. This is consistent with future commercial models [6].

This type of wire in the form of horizontal-spiral outperforms other possible coils in this study in terms of magnetic intensity and AC resistance.

This study shows the inner diameter is an application-specific parameter. It must be noted that the number of turns are constant while inner and outer diameters change in these experiments.

Number of possible coils could be managed by categorization in terms of inner diameter and optimizing other parameters such as number of turns, wire and winding. This suggest the number of turns which is normally an optimization parameter could follow some standards with respect to the wire and winding as well as other manufacturing parameters such as soldering and connections.

Future research will examine actual coils and 3D coil combinations.

REFERENCES

[1] E. Wassermann, C. Epstein, and U. Ziemann, *Oxford Handbook of Transcranial Stimulation*, Oxford press, 2008.
 [2] D. Cohen. And B.N. Cuffin, Developing a more focal magnetic stimulator, Part I: Some basic principles, *Journal of Clinical Neurophysiology*, 8:102-111, 1991.

[3] A. Thielscher, and T. Kammer, Linking physics with physiology in TMS: a spherical field model to determine the cortical stimulation site in TMS, *Neuroimaging*, 17:1117-1130, 1991.

[4] E. Cheng, Computation of the AC resistance of multistranded conductor inductors with multilayers for high frequency switching converters, *IEEE Transactions on Magnetics*, 36:831-834, 2000.

[4] J. Jin, *The Finite Element Method in Electromagnetics*, 2nd Edition, Wiley-IEEE Press, 2002.

[5] C.R. Sullivan, “Cost-constrained selection of strand wire and number in a *Litz*-wire transformer winding”, *IEEE Transactions on Power Electronics*, 16:281–288, 2001.

[6] New England Wire Technologies, www.newenglandwire.com, NH, USA.

[7] B-COOL35, Manufacturer: MagVenture Co., www.MagVenture.com, Farum, Denmark.

[8] L. Xia, G. Shou F. Liu, M. Zhu, Y. Li, S. Crozier, , MRI coil design using boundary element method with regularization technique: a numerical calculation study, *IEEE Transaction on Magnetics*, doi: 10.1109/TMAG.2009.2037753, 2009.

Table 1: Simulation parameters and results. Ro: round, Sq: square: Re: rectangular, S: spiral, H-S: horizontal spiral, V-S: vertical spiral.

| Coil type - Feature | #1 | #2 | #3 | #4 |
|--|------------------|------------------|------------------|------------------|
| Wire/Copper-Film Insulation | Ro | Sq | Re | Re |
| Winding | S | S | H-S | V-S |
| Voltage/Current Single (ohms) | 0.210+i 0.379 | 0.329+i 0.750 | 0.314+i 0.859 | 0.296+i 0.749 |
| Voltage/Current B- <i>Litz</i> (ohms) | 1.301+i 0.821 | 1.521+i 0.762 | 1.289+i 0.837 | 1.256+i 0.650 |
| Voltage/Current C- <i>Litz</i> (ohms) | 0.274+i 0.437 | 0.379+i 0.392 | 0.368+i 0.711 | 0.353+i 0.663 |
| Max. Eddy Ripple ID 1 cm Single (A/mm ²) | 246.37 | 154.06 | 273.53 | 281.92 |
| Max. Eddy Ripple ID 1 cm B-C- <i>Litz</i> (A/mm ²) | 0.000 | 0.000 | 0.000 | 0.000 |
| Max. Magnetic Intensity ID 1 cm (A/m) | 1.2e6 | 1.6e6 | 1.8e6 | 1.5e6 |
| Max. Eddy Ripple ID 2 cm Single (A/mm ²) | 259.13 | 167.43 | 298.12 | 309.07 |
| Max. Eddy Ripple ID 2 cm B-C- <i>Litz</i> (A/mm ²) | 0.000 | 0.000 | 0.000 | 0.000 |
| Max. Magnetic Intensity ID 2 cm (A/m) | 1.5e6 | 1.7e6 | 2.1e6 | 1.9e6 |
| Max. Eddy Ripple ID 3 cm Single (A/mm ²) | 278.23 | 195.76 | 321.26 | 343.91 |
| Max. Eddy Ripple ID 3 cm B-C- <i>Litz</i> (A/mm ²) | 0.000 | 0.000 | 0.000 | 0.000 |
| Max. Magnetic Intensity ID 3 cm (A/m) | 1.8e6 | 1.9e6 | 2.4e6 | 2.2e6 |